The PI3K p110α isoform regulates endothelial adherens junctions via Pyk2 and Rac1

Robert J. Cain,[1] Bart Vanhaesebroeck,[2] and Anne J. Ridley[1]

[1]Randall Division of Cell and Molecular Biophysics, King's College London, London SE1 1UL, England, UK
[2]Centre for Cell Signalling, Institute of Cancer, Queen Mary, University of London, London EC1M 6BQ, England, UK

Endothelial cell–cell junctions control efflux of small molecules and leukocyte transendothelial migration (TEM) between blood and tissues. Inhibitors of phosphoinositide 3-kinases (PI3Ks) increase endothelial barrier function, but the roles of different PI3K isoforms have not been addressed. In this study, we determine the contribution of each of the four class I PI3K isoforms (p110α, -β, -γ, and -δ) to endothelial permeability and leukocyte TEM. We find that depletion of p110α but not other p110 isoforms decreases TNF-induced endothelial permeability, Tyr phosphorylation of the adherens junction protein vascular endothelial cadherin (VE-cadherin), and leukocyte TEM. p110α selectively mediates activation of the Tyr kinase Pyk2 and GTPase Rac1 to regulate barrier function. Additionally, p110α mediates the association of VE-cadherin with Pyk2, the Rac guanine nucleotide exchange factor Tiam-1 and the p85 regulatory subunit of PI3K. We propose that p110α regulates endothelial barrier function by inducing the formation of a VE-cadherin–associated protein complex that coordinates changes to adherens junctions with the actin cytoskeleton.

Introduction

Endothelial cells lining blood vessels provide a barrier between the blood and the tissues. Movement of solutes, nutrients, cytokines, and leukocytes across endothelial cells can occur through both paracellular and transcellular pathways, in which molecules and cells pass either between or through cells, respectively (Engelhardt and Wolburg, 2004; Millán and Ridley, 2005; Nourshargh and Marelli-Berg, 2005).

Endothelial cell–cell contacts comprise tight and adherens junctions similar to those found between adjacent epithelial cells but also contain some proteins unique to endothelial cells, including vascular endothelial cadherin (VE-cadherin), PECAM-1, and ICAM-2 (Dejana et al., 2008). The transmembrane VE-cadherin is a key regulator of endothelial barrier function. VE-cadherin–null mice are embryonic lethal because of defects in vascular development (Carmeliet et al., 1999), and VE-cadherin–blocking antibodies cause a dramatic increase in endothelial permeability in adult mice (Corada et al., 1999). In vitro, inhibition of VE-cadherin increases endothelial permeability and enhances neutrophil transendothelial migration (TEM; Hordijk et al., 1999). VE-cadherin dimers link adjacent cells via homophilic interactions between their extracellular domains, while associating via their cytoplasmic domain with a macromolecular complex that comprises scaffolding and adaptor proteins such as β- and p120-catenin and plakoglobin (Gumbiner, 2005; Dejana et al., 2008).

Many different inflammatory agents induce dynamic changes to endothelial junctions to increase movement of solutes and leukocytes. Proinflammatory cytokines such as TNF and IL-1β induce a gradual increase in vascular permeability, which is sustained for many hours after stimulation. In contrast, other agents such as histamine or thrombin stimulate acute but short-lived changes in permeability. TNF and other inflammatory mediators induce Tyr phosphorylation of VE-cadherin, β-catenin, and/or p120-catenin (Esser et al., 1998; Shasby et al., 2002; Hudry-Clergeon et al., 2005; Angelini et al., 2006). Tyr phosphorylated VE-cadherin acts as a signaling hub to regulate endothelial barrier function by recruiting multiple signaling molecules such as Src, Pyk2, PAK (p21-activated kinase), and

Correspondence to Anne J. Ridley: anne.ridley@kcl.ac.uk

Abbreviations used in this paper: GAPDH, glyceraldehyde 3-phosphate dehydrogenase; GEF, guanine nucleotide exchange factor; HUVEC, human umbilical vein endothelial cell; PI3K, phosphoinositide 3-kinase; TEM, transendothelial migration; TER, transendothelial resistance; VE-cadherin, vascular endothelial cadherin.

The Rockefeller University Press $30.00
J. Cell Biol. Vol. 188 No. 6 863–876
www.jcb.org/cgi/doi/10.1083/jcb.200907135

Tiam-1 (van Buul et al., 2005; Bäumer et al., 2006; Allingham et al., 2007; Turowski et al., 2008). Proinflammatory mediators also stimulate changes in cell shape and actin stress fiber reorganization (Essler et al., 1998; Hordijk et al., 1999), which are proposed to aid junctional disruption during paracellular TEM by increasing tensile force on cell–cell junctions (Wojciak-Stothard and Ridley, 2002; Millán and Ridley, 2005). Several signaling pathways have been implicated in these responses, including the Rho GTPases Rho and/or Rac, the Rho target ROCK (Rho-associated, coiled-coil–containing kinase), Src kinases, and phosphoinositide 3-kinases (PI3Ks; Vouret-Craviari et al., 1998; Wójciak-Stothard et al., 1998; Lampugnani et al., 2002; van Wetering et al., 2003; Birukova et al., 2005; Kilic et al., 2006; Birukov, 2009; Hu and Minshall, 2009).

PI3Ks affect multiple steps of the inflammatory process, including leukocyte TEM (Carman and Springer, 2004; Puri et al., 2004, 2005; Nakhaei-Nejad et al., 2007; Li et al., 2008; Serban et al., 2008). Class I (A and B) PI3Ks consist of a 110-kD catalytic subunit and a regulatory subunit. Class IA comprises three catalytic isoforms, p110α, -β, and -δ, bound to one of five regulatory subunits (p85α and -β, p55α and -γ, and p50α), whereas class IB comprises the p110γ catalytic isoform bound to either a p101 or p84 regulatory subunit (Suire et al., 2005; Cain and Ridley, 2009). Class 1A isoforms are usually activated by binding of the regulatory subunit to Tyr phosphorylated proteins, whereas class 1B PI3K is activated by G protein–coupled receptors (Vanhaesebroeck et al., 2001). Studies in gene-targeted mice have shown that class 1A PI3Ks, particularly p110α, are important for vascular development and angiogenesis (Graupera et al., 2008; Yuan et al., 2008), but whether they regulate endothelial junction integrity has not been studied.

In this study, we investigate the roles of each of the class I PI3K isoforms in endothelial barrier function and leukocyte TEM using siRNA and identify a key role for p110α in these processes through downstream effects on VE-cadherin Tyr phosphorylation, the Tyr kinase Pyk2, and the GTPase Rac.

Results

p110α regulates junctional morphology in endothelial cells

To investigate the roles of class I PI3K isoforms in regulating endothelial junctions, human umbilical vein endothelial cells (HUVECs) were transfected with siRNAs targeting p110α, -β, -γ, or -δ. Knockdown of each isoform did not affect the expression levels of the other isoforms or the regulatory subunit p85 (Fig. 1 A and Fig. S1, A and B). As a readout for PI3K activity, we monitored Akt phosphorylation at residues Ser473 and Thr308 (Vanhaesebroeck and Alessi, 2000; Vanhaesebroeck et al., 2001). Knockdown of p110α, -β, and -γ significantly reduced Akt phosphorylation (Fig. 1 A and Fig. S1 C). The strongest reduction was observed after p110α depletion, which is consistent with observations in VEGF-stimulated mouse endothelial cells (Graupera et al., 2008), whereas p110δ siRNA only had a small effect on total Akt phosphorylation, reflecting the very low levels of this isoform in endothelial cells (Graupera et al., 2008).

Control endothelial cells had a round cobblestone-like morphology with bundles of actin filaments predominantly around the edges of the cells (Fig. 1 B). VE-cadherin and PECAM-1 were localized linearly along cell–cell borders (continuous junctions; Fig. 1 B, arrow) and with a broader distribution where adjacent cells overlapped (overlapping junctions; Fig. 1 B, arrowheads); in these regions, VE-cadherin often had a unique reticular distribution (Fig. 1 B, boxed region in control; and Fig. S2 A; Lampugnani et al., 1995; Noria et al., 1999). As a measure of overlapping junctions, we used VE-cadherin staining to determine the junctional area per cell (junctional index; Fig. S2 B). Depletion of p110α but not p110β, -γ, or -δ increased the level of overlapping junctions (Fig. 1, B and C). This was not caused by a change in the shape of the cells because neither the spread area nor the circularity (circularity = 1 for a circle) were altered (Fig. 1, D and E).

p110α regulates endothelial responses to TNF

We have previously shown that TNF induces a progressive disruption of endothelial cell junctions and an increase in endothelial permeability and stress fibers over 8–24 h after stimulation (McKenzie and Ridley, 2007). TNF is also well known to induce endothelial elongation (Stolpen et al., 1986). Therefore, we investigated whether PI3Ks were activated by TNF and whether they affected TNF-induced responses. TNF transiently increased PI3K activity, as measured by Akt phosphorylation, at 10–30 min, which returned to basal levels at 60 min. It then gradually increased to 12–18 h (Fig. 2 A). This gradual increase correlated well with the time course of changes in endothelial cell morphology and cell–cell junctions (McKenzie and Ridley, 2007).

Cells treated with TNF for 18 h became elongated, and junctions were disrupted, particularly at the ends of elongated cells where VE-cadherin became fragmented (Figs. 2 B and 3, A and C; circularity index). p110α depletion inhibited cell elongation and increased overlapping adherens junctions by over twofold as well as inducing a small increase in cell spread area (Figs. 2 B and 3, B and D; junctional index). In addition, the levels of PECAM-1 and the tight junction marker ZO-1 were higher at junctions after p110α depletion (Figs. 2 B and 3 A). This indicates that junctions are strengthened when p110α is inhibited. These changes were not the result of altered expression of junctional proteins (Fig. S3 A). In contrast to p110α suppression, depletion of p110β, -γ, or -δ did not affect TNF-induced changes to cell–cell junctions or cell shape (Fig. 3, B–D; and Fig. S4, A and B). p110α depletion did not block all TNF-induced signaling because it did not affect early p38MAPK phosphorylation (5–60 min; Fig. S3 B). Interestingly, p110α expression increased gradually over 18 h after TNF addition (Fig. S3 C), which could contribute to the progressive changes to endothelial morphology and junctions.

In addition to alterations to cell–cell junctions and cell shape, TNF induced a dramatic increase in actin stress fibers aligned in parallel bundles along the longest axis of the

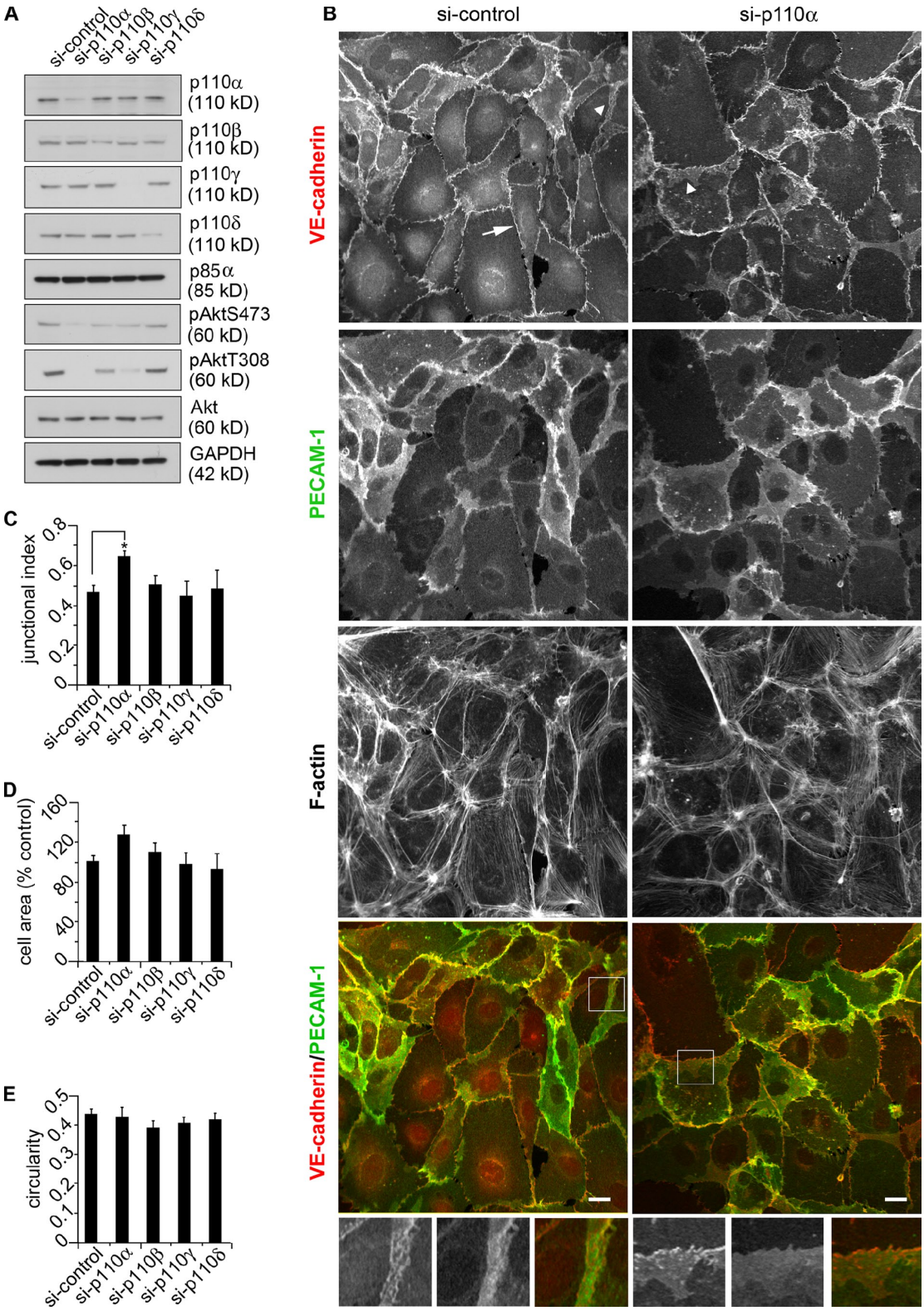

Figure 1. **Inhibition of p110α increases junctional overlap in endothelial cells.** (A) p110 siRNA–transfected HUVECs were lysed and analyzed by SDS-PAGE and blotting for PI3K subunits and Akt phosphorylation. siRNA oligonucleotides specifically knock down only individual isoforms and do not affect levels of the regulatory p85α subunit. GAPDH was used as a loading control. (B) Immunofluorescence micrographs of HUVECs transfected with p110α or control siRNA. Samples were stained with antibodies to VE-cadherin and PECAM-1 and Alexa Fluor 633–conjugated phalloidin to visualize F-actin. The arrow and arrowheads point to examples of linear and overlapping junctions, respectively. Bottom panels are magnifications of the boxed regions (merged images), showing detail of overlapping junctions. (C–E) Junctional index (junctional area/cell number; C), cell area (D), and cell circularity (E) were determined from immunofluorescence images using ImageJ software. In each case, a minimum of five fields were quantified (~20 cells per field) per experiment, and data represent the mean and SEM of at least three independent experiments. Statistical significance was assessed by the Mann-Whitney *U* test; *, $P < 0.05$. Bars, 20 μm.

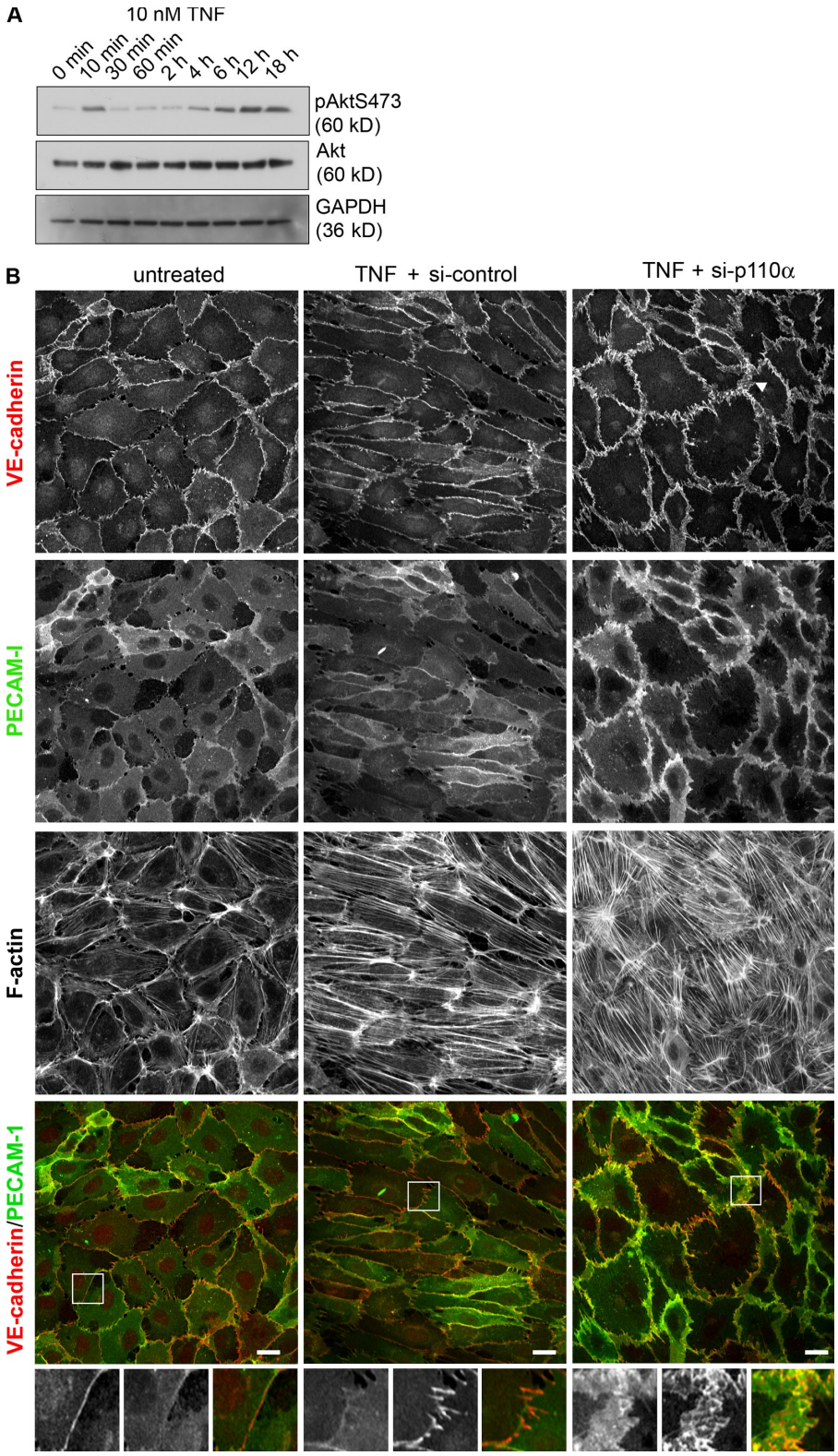

Figure 2. **Inhibition of p110α affects cell–cell junctions and cell morphology after TNF-mediated inflammation.** (A) HUVECs were either stimulated with TNF (10 min to 18 h) or left unstimulated before lysis, SDS-PAGE, and Western blotting with pAktS473, Akt, and GAPDH antisera. (B) Immunofluorescence micrographs of HUVECs transfected with p110α or control siRNA and either stimulated with TNF (18 h) or left unstimulated before fixation. Samples were stained with antibodies to VE-cadherin and PECAM-1 and Alexa Fluor 633–conjugated phalloidin to visualize F-actin. Bottom panels are magnifications of the boxed regions (merged images), showing detail of a linear junction (untreated), disrupted junctions at the boundary of two elongated cells (TNF + si-control), or overlapping junctions (TNF + si-p110α). The arrowhead shows an example of an overlapping junction. Bars, 20 µm.

cell (Fig. 2 B; McKenzie and Ridley, 2007). In cells depleted of p110α, TNF still stimulated an increase in stress fibers, although they were no longer aligned in the same direction in adjacent cells and thus unlikely to exert tension on junctions at the ends of cells (Fig. 2 B). Therefore, a PI3K-independent, TNF-stimulated pathway regulates stress fiber assembly.

p110α regulates endothelial permeability

Endothelial permeability is regulated by cell–cell junctions, and thus, we investigated whether the effect of p110α depletion on junctional organization correlated with a change in endothelial barrier function. TNF treatment progressively increased endothelial permeability to FITC-dextran, with an

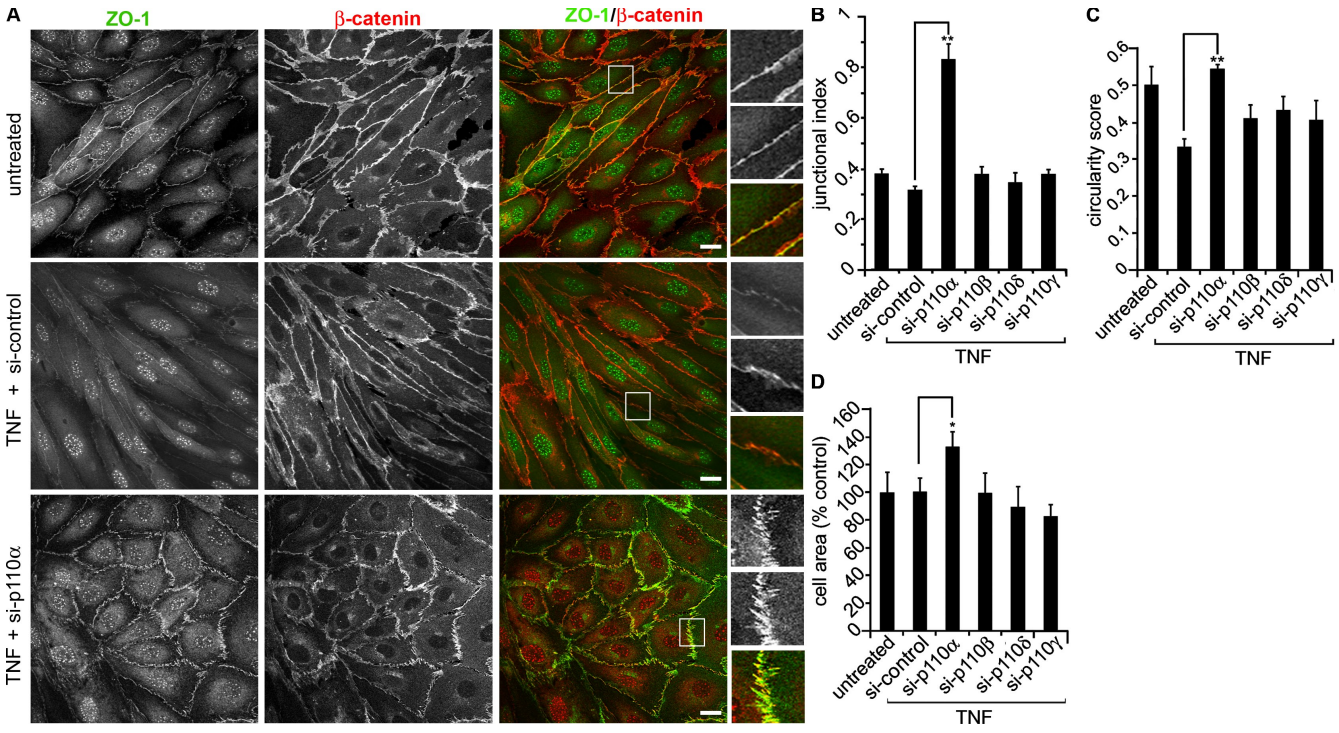

Figure 3. **Inhibition of p110α increases junctional index, cell area, and cell circularity.** (A) Immunofluorescence micrographs of HUVECs transfected with p110α or control siRNA and either stimulated with TNF (18 h) or left unstimulated, before fixation. Samples were stained with antibodies to ZO-1 and β-catenin. Right panels are magnifications of the boxed regions (merged images), showing detail of cell–cell junctions. (B–D) Junctional index (junctional area/cell number; B), cell circularity (C), and area (D) were determined from immunofluorescence images using ImageJ software. In each case, a minimum of five fields were quantified (~20 cells per field) per experiment, and data represent the mean and SEM of at least three independent experiments. Statistical significance was assessed by the Mann-Whitney *U* test; *, $P < 0.05$; **, $P < 0.02$. Bar, 20 µm.

approximately twofold increase at 18 h (Fig. 4 A; McKenzie and Ridley, 2007). p110α suppression with siRNA strongly reduced TNF-induced endothelial permeability (Fig. 4 A), whereas a small decrease was observed for p110γ but not p110δ- or p110β-depleted cells.

We also used transendothelial resistance (TER) to measure the intrinsic barrier function of endothelial monolayers. The TER of HUVECs treated with TNF was ~25% lower than unstimulated cells (Fig. 4 B). In agreement with the permeability data, cells depleted of p110α showed a significant increase in TER compared with controls (Fig. 4 B), whereas knockdown of the other p110 isoforms had no effect. As a positive control, VE-cadherin depletion also reduced resistance (Fig. 4 B), as previously reported (van Gils et al., 2009). In unstimulated cells, p110α depletion also led to an increase in TER (Fig. 4 C), correlating with the increase in overlapping junctions (Fig. 1 C).

Endothelial p110α regulates leukocyte TEM

Leukocytes can cross the endothelium either through the junctions (paracellular TEM) or through the endothelial cells (transcellular route). Endothelial junctional integrity is known to affect leukocyte paracellular TEM (Aghajanian et al., 2008). To assess whether PI3K inhibition affected leukocyte TEM, we initially measured TEM of THP-1 cells, a monocyte-like cell line which only utilizes the paracellular route in vitro (Fig. 5 A and not depicted). There was a significant reduction in THP-1 TEM across p110α-depleted HUVECs, whereas p110β and -γ did not affect TEM. Interestingly, p110δ depletion induced a small reduction in TEM, which could reflect its postulated role in the selectin-mediated tethering of leukocytes to endothelial cells (Puri et al., 2004). To determine whether PI3Ks also affected transcellular TEM, we analyzed diapedesis of T cell lymphoblasts, which use both paracellular and transcellular pathways (Millán et al., 2006). The proportion of T lymphoblasts using the paracellular pathway was significantly reduced across p110α-depleted HUVECs, whereas transcellular TEM remained unaffected, which is consistent with a role for p110α in junctional regulation (Fig. 5 B). Transcellular TEM represented around 15% of TEM events, as previously observed (Millán et al., 2006), and was not affected by suppression of any p110 isoform.

To determine which step of leukocyte TEM was affected by p110α, we used a 3D assay system of HUVECs cultured on a thick collagen gel (Fig. 5 C). Depletion of endothelial cell p110α did not alter leukocyte adhesion after 10 or 60 min, and thus, differences in TEM were not caused by reduced cell attachment (Fig. 5, C and D). Indeed, expression of ICAM-1, a major leukocyte adhesion receptor up-regulated upon TNF stimulation, was not affected by p110α depletion (Fig. S1 A). Endothelial ICAM-1 is known to cluster around some adherent leukocytes (Barreiro et al., 2002; Carman and Springer, 2004), but this clustering was not affected by p110α levels (Fig. S4, C and D). However, p110α depletion reduced the number of cells able to transmigrate across the endothelium into the collagen gel matrix after 1 h (Fig. 5, C and E). Most adherent leukocytes on p110α siRNA–treated HUVECs appeared unable

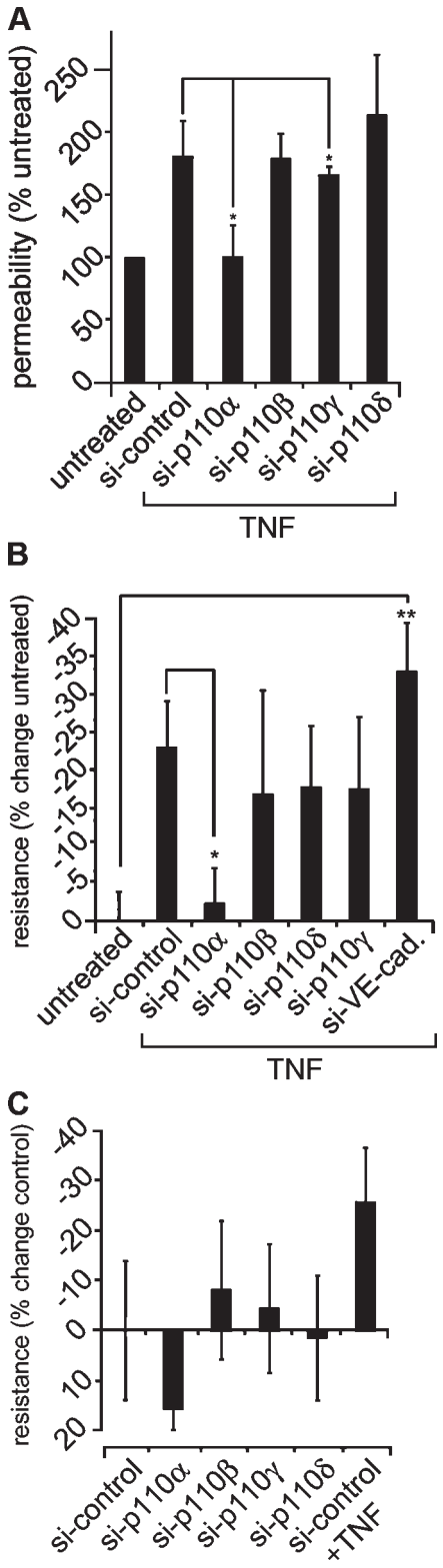

Figure 4. **Inhibition of p110α increases barrier function in TNF-stimulated endothelial cells.** (A) p110 siRNA–transfected HUVECs were either TNF-stimulated (16–18 h; A) or unstimulated before permeability to FITC-dextran was assessed. (B and C) TNF-stimulated (B) and unstimulated (C), p110 siRNA– or VE-cadherin siRNA–transfected HUVECs were seeded at confluence in ECIS electrode chambers, and TER was measured (15 V; 12 h; sampling every 10 min). Data from a stable TER period of 4–6 h were used to calculate mean resistance, and comparisons were made with unstimulated monolayers (assigned as 100%). Mean change in resistance from control is shown. Data represent the mean and SEM of three independent experiments performed in triplicate. Statistical significance was assessed by the Mann-Whitney *U* test; *, $P < 0.05$; **, $P < 0.02$.

to cross endothelial junctions, as determined by staining with β-catenin (unpublished data). For those leukocytes that did cross the endothelium, their ability to invade the collagen matrix was similar (unpublished data), indicating that p110α depletion in endothelial cells does not alter leukocyte migration properties.

p110α inhibition reduces VE-cadherin Tyr phosphorylation

Tyr phosphorylation of VE-cadherin is believed to be an important factor in regulating vascular permeability and correlates with impaired barrier function (Dejana et al., 2008). TNF induced VE-cadherin Tyr phosphorylation (Fig. S5 A), which is consistent with previous observations (Angelini et al., 2006). p110α depletion reduced Tyr phosphorylation of VE-cadherin in TNF-stimulated cells (Fig. 6 A). Several Tyr residues in the VE-cadherin intracellular domain can be phosphorylated, including Y731, Y658, and Y685 (Allingham et al., 2007; Wallez et al., 2007; Turowski et al., 2008). To assess whether the p110α-regulated changes in total VE-cadherin phosphorylation were caused by one or more of these residues, lysates were blotted with phosphospecific antibodies for each of these sites. p110α siRNA–treated cells showed a strong reduction in Y731 phosphorylation and a smaller reduction at Y658 but no change at Y685 (Fig. 6 A), indicating that p110α regulates VE-cadherin Tyr phosphorylation on specific sites. It is also possible that the pY731 antibody recognizes other phospho-Tyr residues on VE-cadherin in addition to pY731 and that p110α regulates phosphorylation of these sites.

p110α depletion reduces Pyk2 activity and its association with VE-cadherin

Both Pyk2 and Src have been identified as potential Tyr kinases involved in the regulation of VE-cadherin phosphorylation (Allingham et al., 2007; Turowski et al., 2008). Pyk2 was present in VE-cadherin immunoprecipitates in unstimulated cells and at higher levels in TNF-stimulated cells, whereas its close relative FAK was not detected (Fig. 6 B and Fig. S5 A). Pyk2 association with VE-cadherin was much reduced in p110α-depleted cells, both in TNF-stimulated and unstimulated cells (Fig. 6 B and Fig. S5). In unstimulated cells, knockdown of p110γ also slightly reduced Pyk2–VE-cadherin association, suggesting that under some circumstances, p110γ could also affect junctional integrity, for example downstream of the G protein–coupled IL-8 receptor (Gavard et al., 2009), although not in the TNF response.

Y402 phosphorylation on Pyk2 reflects Pyk2 kinase activity (Mitra et al., 2005). TNF induced a small increase in pY402-Pyk2 at around 60 min and a larger increase at 12–18 h (Fig. 7), correlating with the delayed increase in PI3K activity induced by TNF (Fig. 2 A). Pyk2 Y402 phosphorylation was reduced by p110α suppression both in VE-cadherin immunoprecipitates and in total lysates, indicating that p110α regulates both Pyk2

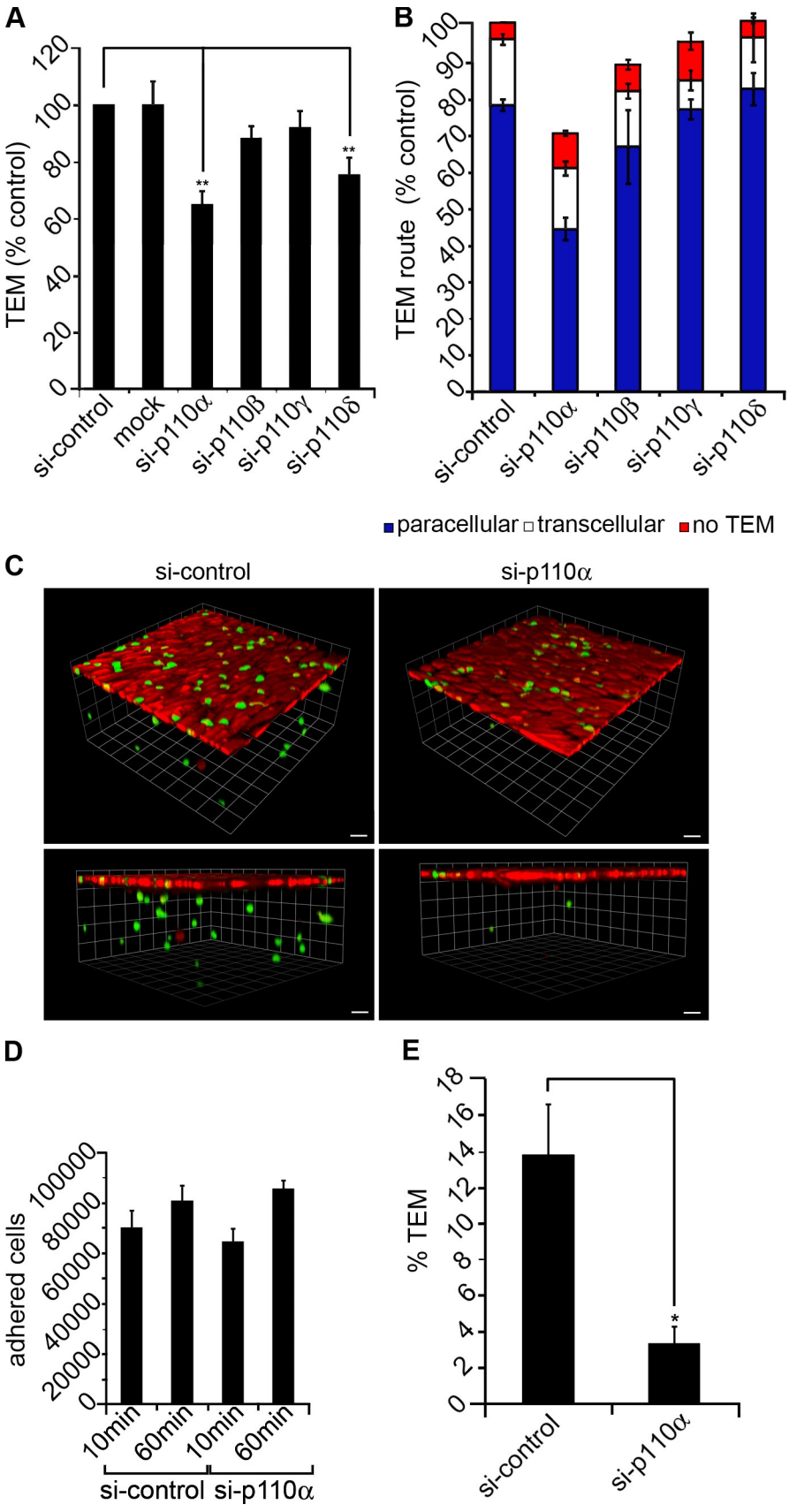

Figure 5. **p110α inhibition in endothelial cells reduces leukocyte TEM.** (A) THP-1 cells were added to TNF-stimulated, siRNA-transfected HUVECs grown in Transwell chambers, and the resultant TEM efficiency toward MCP-1 was determined after 1 h. (B) T lymphoblasts were added to TNF-stimulated, siRNA-transfected HUVECs and fixed after 15 min. Samples were analyzed by confocal microscopy and scored visually for paracellular and transcellular TEM events (Millán et al., 2006). (C) TNF-stimulated, p110α siRNA– or control siRNA–transfected HUVECs previously labeled with CellTracker orange dye were grown on collagen matrices in Transwell chambers. CellTracker green–labeled THP-1 cells were added to HUVECs, and TEM was allowed to proceed toward an MCP-1 gradient in the lower chamber for either 10 or 60 min before fixation; confocal z stacks were then collected. 3D reconstructions were produced using Volocity software. A small gamma correction was applied to the red channel to visualize weak cell tracker staining at the edges of cell, which are difficult to distinguish upon 3D rendering. (D and E) Quantification of adhesion to endothelial cells (D) or TEM (THP-1 cells within the collagen matrix; E). Results represent the mean and SEM of at least three independent experiments. Statistical significance was assessed by the Mann-Whitney *U* test; *, $P < 0.05$; **, $P < 0.02$. Bars, 40 μm.

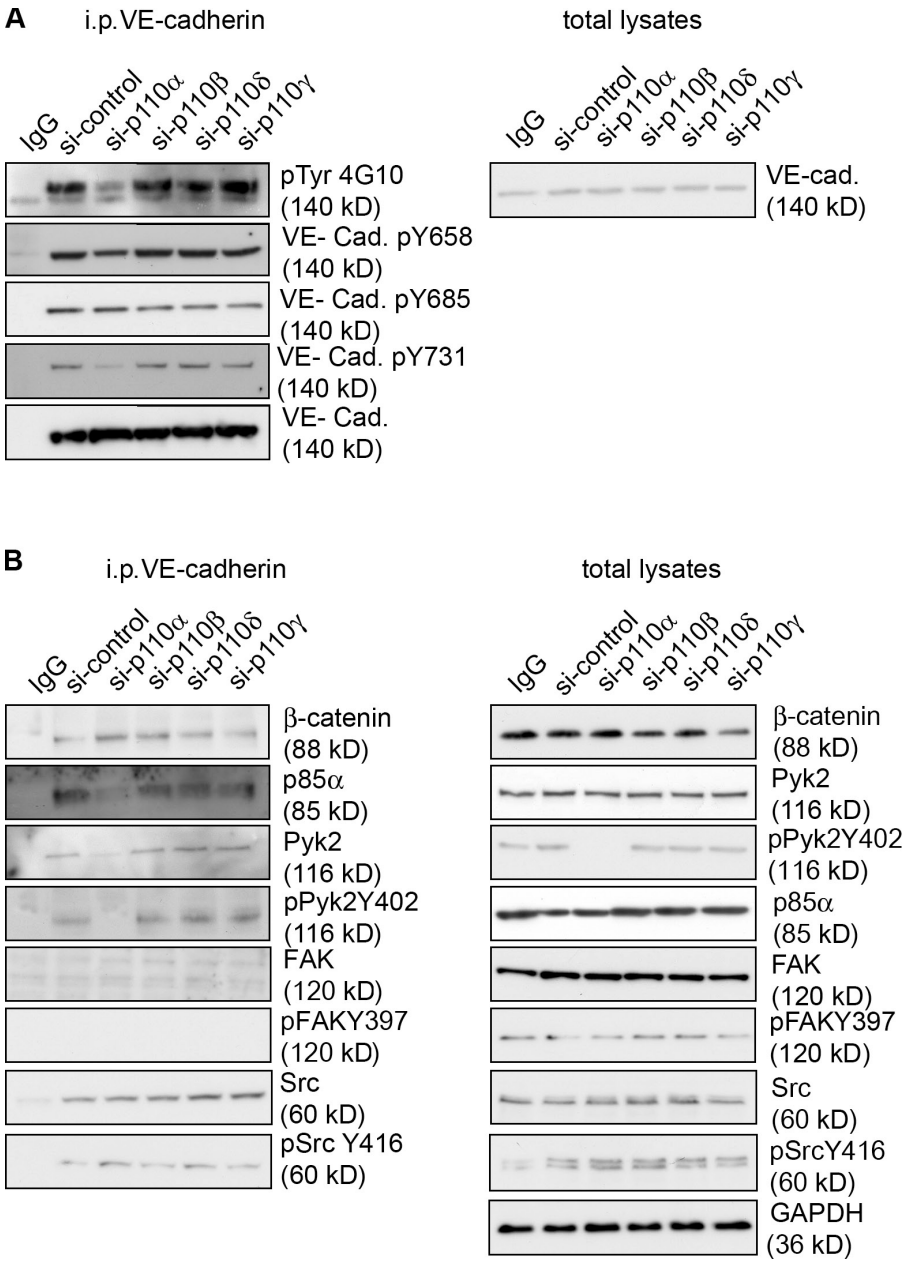

Figure 6. **Inhibition of p110α reduces VE-cadherin Tyr phosphorylation and Pyk2 activity.** (A and B) TNF-stimulated, siRNA-transfected HUVECs were lysed, and VE-cadherin was immunoprecipitated (i.p.). Samples were separated by SDS-PAGE and analyzed by Western blotting with antibodies to total phospho-Tyr and for VE-cadherin phosphorylated at Y658, Y685, and Y731 (A) and other proteins as indicated (B). Total lysates were probed in parallel (blots on right) to control for variations in protein level.

association with VE-cadherin and Pyk2 activation. Src was also detected in VE-cadherin immunoprecipitates, but unlike Pyk2, neither its levels nor its activity, as measured with antibodies to pY416-Src (Parsons and Parsons, 2004), were affected by p110 depletion (Fig. 6 B). p110α depletion did not induce reduced VE-cadherin binding to all its partners because the levels of β-catenin coimmunoprecipitated with VE-cadherin were not affected (Fig. 6 and Fig. S5 A).

The p85 subunit of PI3K has previously been reported to associate with Tyr phosphorylated VE-cadherin, which could be via p85 SH2 domains (Hudry-Clergeon et al., 2005). The level of p85 coimmunoprecipitation with VE-cadherin was increased by TNF stimulation (Fig. 6 B and Fig. S5 A), reflecting the higher VE-cadherin Tyr phosphorylation. The amount of p85 immunoprecipitated with VE-cadherin was strikingly reduced after p110α depletion, both with and without TNF stimulation (Fig. 6 B and Fig. S5 A), suggesting that PI3K-α activity itself regulates p85 association with VE-cadherin by increasing VE-cadherin Tyr phosphorylation.

Knockdown of p110α reduces Rac1 and RhoA activity

Rho GTPases are important regulators of endothelial barrier function (Wojciak-Stothard and Ridley, 2002; Fryer and Field, 2005; Tzima, 2006), and VE-cadherin has been implicated in the regulation of Rac1 activity (Lampugnani et al., 2002). In addition, PI3K isoforms affect Rho GTPase activity in endothelial and other cells (Papakonstanti et al., 2007; Graupera et al., 2008; Cain and Ridley, 2009). Therefore, we investigated whether p110α knockdown affected Rho, Rac, or Cdc42 activity. Despite being implicated in epithelial barrier function (Bruewer et al., 2004), active Cdc42 levels were not affected by

p110 knockdown (Fig. 8 A). In contrast, Rac1 and RhoA activities were both dramatically reduced in p110α-depleted HUVECs but not by knockdown of the other PI3K isoforms. Interestingly, of the Rho isoforms, only the level of GTP-RhoA was affected by p110α but not GTP-RhoB or -RhoC (Fig. 8 B).

VE-cadherin regulates the localization of the Rac guanine nucleotide exchange factor (GEF) Tiam-1 to endothelial cell–cell junctions (Lampugnani et al., 2002), and PI3Ks regulate Tiam-1 localization through its N-terminal pleckstrin homology domain (Sander et al., 1998). To assess whether PI3K-mediated changes in Rac1 or RhoA activity were linked to VE-cadherin, VE-cadherin immunoprecipitates from p110α-depleted HUVECs were probed for the Rac GEFs Tiam-1 and Vav and the Rho GEF GEF-H1, which has previously been reported to localize to endothelial junctions (McKenzie and Ridley, 2007). Although Vav and GEF-H1 could not be detected (not depicted), Tiam-1 associated with VE-cadherin in both unstimulated and TNF-stimulated endothelial cells, and levels were lower in p110α-depleted HUVECs (Fig. 8 C and Fig. S5). This suggests that p110α mediates Rac1 activation by regulating Tiam-1 association with VE-cadherin.

Rac1 and Pyk2 regulate endothelial barrier function and leukocyte TEM

Because p110α regulates both Rac1 and Pyk2 activities, we investigated whether they contributed to p110α-regulated barrier function in endothelial cells using siRNA to knock down their expression (Fig. 9 A). Both Pyk2 and Rac1 depletion reduced TNF-induced endothelial permeability (Fig. 9 B), whereas RhoA knockdown had no effect (Fig. S5). In addition, knockdown of Pyk2 or Rac1 in HUVECs reduced THP-1 TEM, and this effect was significant when both Pyk2 and Rac1 were depleted (Fig. 9 D). Interestingly, Pyk2 and Rac1 each had different effects on endothelial morphology that could affect barrier function. Like p110α suppression, Pyk2-depleted cells had an increase in overlapping cell junctions and junctional index, both in stimulated and unstimulated cells, whereas Rac1 knockdown did not affect junctional index (Fig. 9 E and not depicted). In contrast, Rac1 and p110α but not Pyk2 depletion inhibited TNF-induced cell elongation (circularity; Fig. 9, C and F), which reduced the disruption of junctions observed at the ends of elongated cells (Fig. 2 B). Knockdown of both Rac1 and Pyk2 inhibited cell elongation and increased overlapping junctions (Fig. 9, E and F), although stress fibers were still induced, which is consistent with results with p110α depletion (Fig. 2 B). These results indicate for the first time that TNF-induced changes to cell shape and junction morphology are regulated separately and that both of these responses are likely to affect barrier function.

Discussion

PI3Ks have been shown to regulate vascular integrity and angiogenesis during development, but the mechanistic basis for their effects on endothelial cells has not been determined. In this study, we have identified a specific role for p110α in regulating endothelial junctions, affecting both TNF-induced endothelial permeability and leukocyte TEM. Our results indicate that p110α acts via VE-cadherin Tyr phosphorylation, the Tyr kinase Pyk2, and the Rho GTPase Rac1 to regulate these responses.

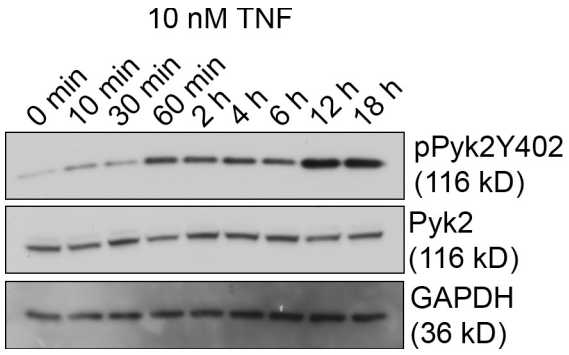

Figure 7. **Pyk2 activity is increased by TNF stimulation.** Endothelial cells were either stimulated with TNF (10 min to 18 h) or left unstimulated before lysis, SDS-PAGE, and immunoblotting with pY402-Pyk2, Pyk2, and GAPDH antisera.

Tyr phosphorylation of the intracellular domain of VE-cadherin leads to protein binding and correlates with increased endothelial permeability and TEM (Lambeng et al., 2005; Potter et al., 2005; Turowski et al., 2008). Our data indicate that p110α plays a key role in the assembly of a VE-cadherin signaling complex by regulating Tyr phosphorylation of VE-cadherin residue Y731, with a smaller effect on Y658. Several kinases contribute to VE-cadherin phosphorylation, including Pyk2 and Src family kinases, and a dominant-negative Pyk2 construct was shown to affect junctional integrity (Weis et al., 2004; van Buul et al., 2005; Allingham et al., 2007; Wallez et al., 2007). In agreement with this, we find that knockdown of Pyk2 reduces both endothelial permeability and leukocyte TEM. We show in this study for the first time that p110α acts upstream of Pyk2 and regulates both Pyk2 autophosphorylation and its association with VE-cadherin. Like its close relative FAK, Pyk2 autophosphorylation recruits Src kinases (Basile et al., 2007). VE-cadherin Y731 is a putative Pyk2 target (Dejana et al., 2008), although it is unclear whether Pyk2 is able to directly phosphorylate VE-cadherin in vivo or whether it acts indirectly, for example by recruiting a Src kinase such as Fyn, which has been reported to mediate TNF-induced Tyr phosphorylation of VE-cadherin (Angelini et al., 2006). As Pyk2 has no SH2 domain, it is unlikely to bind directly to phosphorylated tyrosines in VE-cadherin, but it could be recruited via the p85 regulatory subunit of PI3K. We show that p85 associates with VE-cadherin and PI3K interacts with Pyk2 (Melikova et al., 2004), probably via the interaction of a p85 SH2 domain with a Pyk2 phospho-Tyr (van Buul et al., 2005; Allingham et al., 2007). Interestingly, p85 interaction with VE-cadherin is reduced by p110α inhibition, presumably because p85 association with the complex depends on PI3K-α–mediated VE-cadherin Tyr phosphorylation.

Our data suggest that p110α regulates Rac activity via recruitment of the Rac GEF Tiam-1 to the VE-cadherin complex. Recruitment of Tiam-1 to membranes in endothelial cells is dependent on VE-cadherin (Lampugnani et al., 2002), and the N-terminal pleckstrin homology domain of Tiam-1

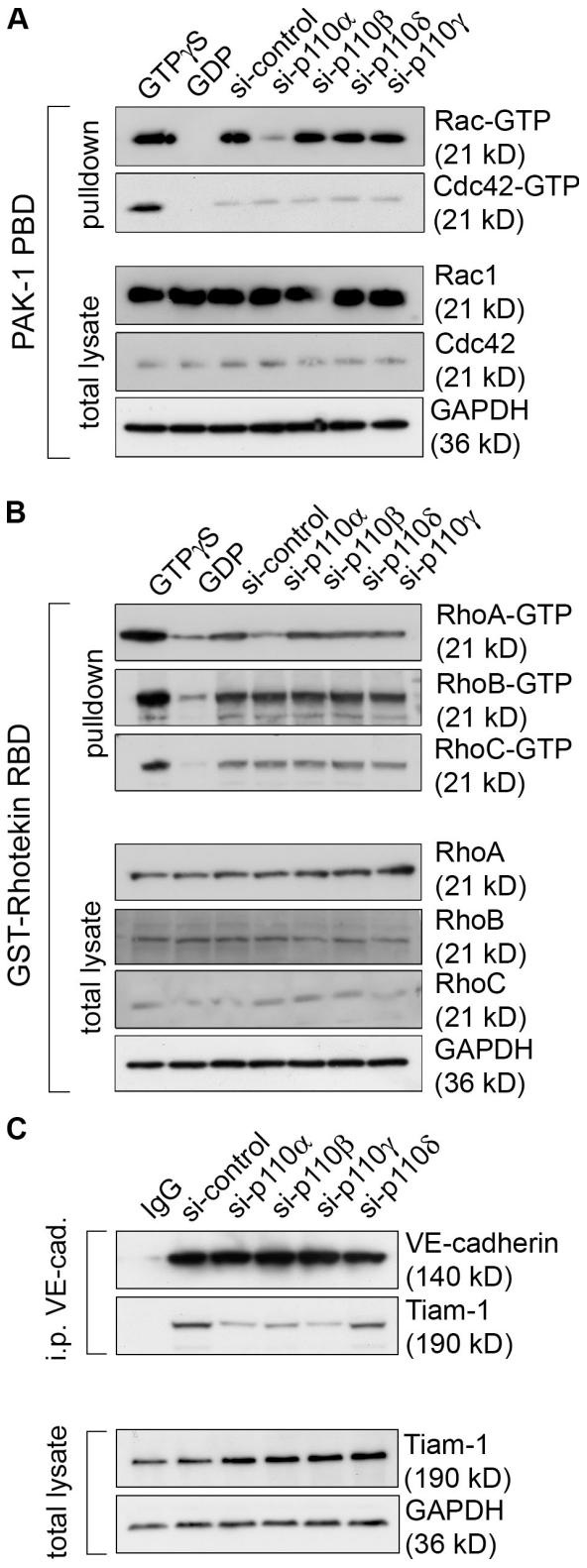

Figure 8. **p110α depletion decreases RhoA and Rac but not Cdc42 activity.** (A and B) TNF-stimulated, p110 siRNA–transfected HUVECs were lysed, and Rho GTPase activity was determined by affinity for GST-Rhotekin-RBD– or GST-PAK1-PBD–conjugated beads for RhoA/B/C and Rac/Cdc42, respectively. After washing, samples were separated by SDS-PAGE and analyzed by Western blotting with antibodies to Rac1 or Cdc42 (A) or RhoA, -B, or -C (B). Total lysates (bottom) of each sample were Western blotted in parallel to control for total amounts of GTPase. GAPDH was used as a loading control. (C) PI3K inhibition reduces Tiam-1 association with VE-cadherin. TNF-stimulated, siRNA-transfected HUVECs were lysed, and VE-cadherin was immunoprecipitated (i.p.). Samples were separated by SDS-PAGE and analyzed by Western blotting with antibodies to Tiam-1. Total lysates (bottom) were probed in parallel to control for variations in protein level. GAPDH was used as a loading control.

binds to $PtdIns_{(3,4,5)}P_3$ (Hordijk et al., 1997; Michiels et al., 1997). Association of p110α via p85 with VE-cadherin might thereby provide a mechanism by which Tiam-1 is recruited and activates Rac1.

p110α inhibition prevents two TNF-induced morphological responses that could be linked to endothelial barrier function, cell junction morphology, and cell elongation via Pyk2 and Rac1, respectively. p110α and Pyk2 depletion both lead to an increase in adherens junction staining, predominantly in regions where endothelial cells overlap. These junction-rich regions are likely to form a strong barrier to both small molecules and leukocytes. In contrast, Rac1 mediates TNF-induced elongation and contributes to permeability and leukocyte TEM, indicating that cell shape affects barrier function. This could be because in elongated cells, stress fibers exert a higher tension on cell–cell junctions and thus decrease junctional integrity at cell poles compared with cells with a more cobblestone shape. Indeed, leukocytes preferentially transmigrate at poles of elongated endothelial cells (Millán et al., 2006), and endothelial shape changes have been proposed to contribute to TNF-induced vascular leakage in vivo (Cotran and Pober, 1990). Interestingly, RhoA-depleted cells did not show a reduction in TNF-induced stress fibers or altered barrier function. This is consistent with our previous results suggesting that TNF-induced stress fiber assembly and endothelial permeability do not correlate with RhoA activation (McKenzie and Ridley, 2007).

Previous studies have suggested that PI3Ks are important for efficient TEM in vivo and in vitro (Puri et al., 2004, 2005; Nakhaei-Nejad et al., 2007). In vitro, treatment of HUVECs with pan-PI3K inhibitors did not affect lymphocyte adhesion but reduced diapedesis. Our results indicate that this step specifically involves p110α. In vivo studies with gene-targeted mice have implicated endothelial p110γ and -δ in selectin-mediated neutrophil tethering and rolling but not ICAM-1–mediated firm attachment to endothelial cells (Puri et al., 2004, 2005), and indeed, we see a small effect of p110δ on leukocyte TEM in our model, which is consistent with an involvement in selectin function. So far, the roles of p110β or -α have not been tested in vivo. Collectively, these results and our data indicate that p110α acts in endothelial cells primarily to regulate changes in junctional integrity induced by TNF and thus influence leukocyte diapedesis, whereas p110γ and -δ are involved in selectin-mediated leukocyte tethering. It is also possible that p110α affects adhesion receptor signaling in some way that reduces subsequent TEM.

In conclusion, we have shown that the p110α isoform of PI3K specifically regulates cell–cell contacts in endothelial cells, thereby contributing to TNF-induced changes to endothelial barrier function and leukocyte TEM. This selective

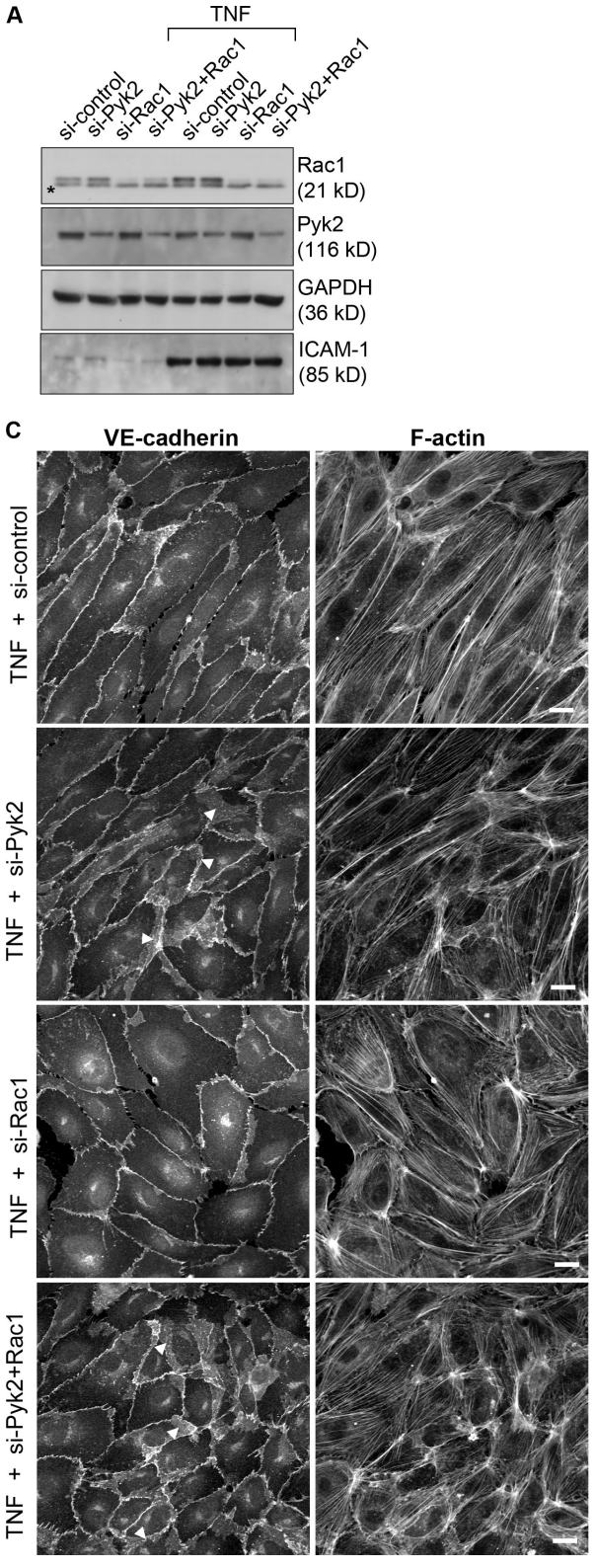

Figure 9. **Pyk2 and Rac1 depletion alter endothelial junctions and leukocyte TEM.** HUVECs were transfected with either control siRNA or siRNA to Pyk2 and/or Rac1 and then stimulated with TNF (18 h) or left unstimulated. (A) HUVECs were lysed and analyzed by SDS-PAGE and Western blotting with Pyk2, Rac1, and GAPDH antibodies to assess siRNA knockdown efficiency and ICAM-1 to assess TNF stimulation. The asterisk indicates a nonspecific band; Rac1 is the top band. (B) Barrier function of siRNA-treated HUVECs either stimulated with TNF (16–18 h) or left unstimulated was assessed by permeability to FITC-dextran. Unstimulated monolayers were assigned as 100%. (C) Immunofluorescence micrographs of siRNA-transfected HUVECs. Samples were stained with antibodies to VE-cadherin and Alexa Fluor 633–conjugated phalloidin to visualize F-actin. Arrowheads indicate examples of overlapping junctions. (D) THP-1 cells were added to siRNA-treated, TNF-stimulated HUVECs in Transwell chambers, and the resultant TEM efficiency toward MCP-1 was determined after 1 h. (E and F) Junctional index (junctional area/cell number; E) and cell circularity (F) were determined from immunofluorescence images. Data represent the mean and SEM of at least four independent experiments, each performed in triplicate. Statistical significance was assessed by the Mann-Whitney *U* test; *, $P < 0.05$; **, $P < 0.02$. Bars, 20 µm.

role of p110α in endothelial cells could in part explain its role to angiogenesis (Graupera et al., 2008), which requires dynamic changes to endothelial cell–cell junctions and shape. Our results suggest that p110α-selective inhibitors could be used to treat chronic inflammatory diseases involving TNF such as arthritis and atherosclerosis.

Materials and methods

Antibodies and reagents

Antibodies to p110α, -β, -γ, and -δ have been previously described (Graupera et al., 2008; Guillermet-Guibert et al., 2008). Antibodies to ZO-1, -2, and -3, JAM-A, occludin, VE-cadherin–Y731, and claudin-5 were purchased from Invitrogen, α- and β-catenin and β-actin were

purchased from Sigma-Aldrich; VE-cadherin, p120-catenin, and phospho–p120-catenin were obtained from BD; RhoA, -B, and -C and Tiam-1 were purchased from Santa Cruz Biotechnology, Inc.; Akt, pAktS473, pAktT308, Pyk2, and Pyk2Y402 were obtained from Cell Signaling Technology; VE-cadherin–Y658, glyceraldehyde 3-phosphate dehydrogenase (GAPDH), and p85 were obtained from Millipore; VE-cadherin–Y685 was purchased from ECM Biosciences; ICAM-1 was obtained from R&D systems; and PECAM-1 was obtained from Dako. FITC-dextran was purchased from Sigma-Aldrich, and TNF was obtained from PeproTech. CellTracker orange and CellTracker green dyes were purchased from Invitrogen.

Cell culture

Pooled HUVECs were purchased from Lonza and cultured in EGM-2 medium (Lonza) containing 3% FCS. Cells were used for experiments between passages 1 and 4 and were seeded onto fibronectin-coated (10 µg/ml; Sigma-Aldrich) flasks, glass coverslips, or filters. For experiments, HUVECs were stimulated with 10 ng/ml TNF for 18 h except where indicated. THP-1 cells were maintained in suspension culture in RPMI 1640 medium (Invitrogen) containing 10% FCS and 2 mM L-Gln at between 5×10^{-5} and 2×10^{-6}/ml. T lymphoblasts were prepared from isolated human peripheral blood mononuclear cells (peripheral blood lymphocytes). After stimulation with 0.5% phytohemagglutinin for 48 h, nonadherent peripheral blood lymphocytes were washed and cultured in RPMI 1640 medium (10% FCS and 2 U/ml IL-2 in 5% CO_2) and used in experiments after culturing for 7–12 d.

siRNA transfection

HUVECs were seeded at 10^5 cells per well in 6-well dishes 24 h before transfection. Four individual siRNA oligonucleotides (Thermo Fisher Scientific) targeting each of the human p110α (D-003018-05, D-003018-06, D-003018-07, and D-003018-08), p110β (D-003019-05, D-003019-06, D-003019-07, and D-003019-09), p110γ (D-005274-03, D-005274-04, D-005274-05, and D-005274-06), or p110δ (D-006775-05, D-006775-06, D-006775-07, and D-006775-08) catalytic subunits or oligonucleotides targeting RhoA (D-003860-01 and D-003860-03), Rac1 (D-003560-05 and D-003560-07), Pyk2 (L-003165-00), or VE-cadherin (D-003641-03) were tested for knockdown activity by Western blotting and subsequently used individually (RhoA, Rac1, Pyk2, and VE-cadherin) or as four oligonucleotide pools. For p110 isoforms, the siRNA pools gave the strongest knockdown and were therefore used in all subsequent experiments. siRNAs diluted in EBM-2 medium without FCS were premixed with EBM-2–diluted Oligofectamine reagent (Invitrogen) as described in the manufacturer's instructions. Cells were transfected (6 h) in 1 ml of EBM-2 medium containing growth supplements, but excluding antibiotics and FCS, giving a final oligonucleotide concentration of between 80 and 200 nM. 1 ml EBM-2 medium with growth factors and 8% FCS was subsequently added to each well, and cells were incubated overnight. After transfection (24 h), cells were trypsinized and plated either at confluence or subconfluence and allowed to adhere (8 h) on fibronectin-coated dishes or coverslips for the different assays.

Immunofluorescence microscopy

HUVECs grown to confluence on glass coverslips were fixed with 3.7% (wt/vol) paraformaldehyde, permeabilized with 0.2% (vol/vol) Triton X-100 in PBS (15 min), blocked with 3% (wt/vol) BSA in PBS (1 h), and then incubated with primary antibodies in 3% BSA in PBS (1 h). Samples were sequentially incubated for 1 h with Alexa Fluor 488– or Alexa Fluor 546–conjugated anti–rabbit or anti–mouse IgG secondary antibodies, followed by incubation with Alexa Fluor 633–conjugated phalloidin (20 min; Invitrogen). Coverslips were mounted using ProLong Antifade reagent (Invitrogen). Images were acquired at room temperature using a confocal microscope (LSM 510 META; Carl Zeiss, Inc.) with three single photomultiplier tube confocal detectors mounted on an inverted microscope (Axio-Observer Z1; Carl Zeiss, Inc.) at a magnification of 40 with an oil immersion objective (EC Plan-Neofluar 40× NA 1.30 oil differential interference contrast M27). Images were processed using Zen software (Carl Zeiss, Inc.), and figures were assembled using Photoshop CS4 (Adobe). Quantification of cell area, circularity, and junctional index (junctional area/cell number) was performed using ImageJ software (National Institutes of Health). Circularity was calculated using the formula $4\pi(\text{area}/\text{perimeter}^2)$. A circularity value of 1 indicates a perfect circle. As the value approaches 0, it indicates an increasingly elongated polygon. Junctional index was calculated using the formula ([junctional area/total area] × 100)/cell number. Junctional area was calculated per field by using the VE-cadherin–stained channel, thresholding the image to create an even intensity stain corresponding to junctional area, and quantifying its area using the software analysis options (Fig. S2 B). In each case, a minimum of five fields were quantified (~20 cells per field) per experiment, and data shown represent the mean of at least three independent experiments.

TEM assay

HUVECs were plated at confluence on Transwell inserts (5-µm pore). After 6–8 h, cells were treated with 10 ng/ml TNF for 18 h. 10 µg/ml MCP-1 was added to the bottom chamber before the addition of 1×10^5 washed THP-1 cells to the upper chamber. Cells were left to transmigrate (1 h; 37°C) before medium from the bottom chamber was removed, and cells were counted using a cell counter (CASY; Innovatis). Each experiment was performed in triplicate. For quantification of T lymphoblast paracellular and transcellular TEM events, T lymphoblasts (provided by E. Cernuda-Morollon, University College London, London, England, UK) were added to confluent TNF-stimulated HUVECs on glass coverslips for 15 min before fixation with 4% paraformaldehyde. Samples were stained with anti–ICAM-1/Alexa Fluor 488–conjugated anti–mouse IgG, anti–β-catenin/Alexa Fluor 546–conjugated anti–rabbit, and Alexa Fluor 633–conjugated phalloidin. T lymphoblasts undergoing TEM were easily distinguishable by confocal microscopy, as the leading edge was in contact with the coverslip, whereas the rear uropod was still localized on the surface of the endothelial cell. β-Catenin and ICAM-1 staining was used to determine whether the cell was undergoing paracellular or transcellular diapedesis, respectively. Each experiment was performed in quadruplicate, quantifying 25 fields per condition.

3D model for TEM

HUVECs were seeded at confluence onto collagen I gels polymerized in 12-µm pore Transwell filters. After 6–8 h, monolayers were treated with 10 ng/ml TNF for 18 h. HUVECs were labeled with 5 µM CellTracker orange for 40 min before washing in normal medium. 10 µg/ml MCP-1 was added to the bottom chamber before the addition of 1×10^4 washed CellTracker green–labeled THP-1 cells to the upper chamber. After 10 or 60 min, HUVECs were washed three times to remove unbound THP-1 cells, and then Transwells were fixed by immersion in 3.7% (wt/vol) paraformaldehyde before being processed for immunofluorescence microscopy. z sections were acquired at 200-nm intervals by confocal microscopy (see Immunofluorescence microscopy), and 3D images were reconstructed using Volocity image analysis software (PerkinElmer). Adhesion and TEM (leukocytes below the level of the endothelial cells) were assessed using ImageJ software to count CellTracker green voxels either above or within the matrix, and cell numbers were determined by comparison with a standard curve of known voxel/cell numbers.

Transendothelial permeability assays

HUVECs were seeded onto 0.4-µm pore Transwell filters (Thermo Fisher Scientific) at confluency. After 6–8 h, monolayers were treated with 10 ng/ml TNF for 18 h. 0.1 µg/ml FITC-dextran (molecular weight, 42,000) was subsequently applied to the apical chamber and allowed to equilibrate for 45 min before a sample of the medium was removed from the lower chamber to measure basal permeability. Fluorescence was measured using a fusion universal microplate analyzer (Fusion-FA; PerkinElmer; excitation, 492 nm; detection, 520 nm), and data were expressed as a ratio of the control untreated monolayer fluorescence. All experiments were performed in triplicate, and results shown are the mean of at least four independent experiments.

TER measurement

Transfected HUVECs were plated at confluence on dishes containing gold electrodes (ECIS; Applied Biophysics). After 24 h, cells were washed in warm EGM-2 media and either treated with 10 ng/ml TNF for 18 h or left untreated before data were collected on a resistance meter (ECIS 1600; Applied Biophysics). Resistance data were collected at a constant voltage of 15 V for a period of 12 h, sampling data every 10 min. Data from a stable period of 4–6 h were used to calculate mean resistance. Control siRNA transfection did not alter the TNF-induced decrease in resistance.

Rho, Rac, and Cdc42 activity assays

Pull-down activity assays were performed using either GST-Rhotekin RBD beads (Cytoskeleton, Inc.; 50 µg per pull-down for Rho) or GST-PAK1 PBD agarose conjugate (Millipore; 10 µg per pull-down for Rac/Cdc42). 7×10^6 cells per condition were lysed rapidly in pull-down buffer (50 mM Tris, pH 7.5, 1% Triton X-100, 0.5% Na deoxycholate, 0.1% SDS, 500 mM NaCl, 100 mM $MgCl_2$, 10 µg/ml leupeptin, 10 µg/ml aprotinin, 1 mM PMSF, 10% glycerol, and 1 mM DTT) before transferring to a microfuge tube (Fresco 17 centrifuge; Thermo Fisher Scientific) and centrifuging (13,000 *g*;

10 min; 4°C). A 50-µl sample of whole cell lysate was retained, and the remaining supernatant was incubated with the appropriate beads (1 h; 4°C with rotation). Beads were washed three times in pull-down buffer and boiled for 5 min in Laemmli sample buffer, and proteins were resolved by SDS-PAGE and Western blotting. Protein loading was determined by reprobing the whole cell lysate lanes with an anti-GAPDH antibody.

Immunoprecipitation and Western blotting

HUVECs were harvested by scraping into lysis buffer (50 mM Tris-HCl, pH 7.4, 1% [vol/vol] NP-40, 150 mM NaCl, 0.25% Na deoxycholate, 1 mM EGTA, 1 mM Na orthovanadate, 1 mM Na fluoride, 1 µM PMSF, and 1 µg/ml each of aprotinin, leupeptin, and pepstatin) and lysed by passing through a 21-gauge needle. Lysates were clarified (10,000 *g*; 10 min; 4°C), and protein concentrations were measured and standardized. VE-cadherin was immunoprecipitated by the addition of anti–VE-cadherin monoclonal antibodies and protein G–conjugated agarose beads (2 h; 4°C). A sample of identically treated control lysates was incubated with agarose-conjugated anti–mouse IgG as a negative antibody control. Beads were sedimented (500 *g*; 1 min) and washed three times with lysis buffer containing an additional 100 mM NaCl. Immunoprecipitated proteins were eluted and boiled in Laemmli buffer containing 0.1 mM DTT. Samples were separated by SDS-PAGE using a gradient gel system (12–15% gradient gels; Invitrogen), transferred to polyvinylidene fluoride membranes (2 h; 50 V), and blocked with 5% nonfat dried milk or 5% BSA in TBS (20 mM Tris-HCl, pH 7.5, and 150 mM NaCl), followed by subsequent incubations with appropriate primary and secondary antibodies in TBS with 5% nonfat dried milk/BSA (1 h or overnight) and washing in TBS-T (TBS with 0.1% Triton X-100). Proteins were detected using the enhanced chemiluminescence detection system (GE Healthcare).

Online supplemental material

Fig. S1 shows the knockdown efficiency of p110 isoforms and effects on Akt phosphorylation. Fig. S2 shows that depletion of p110β, -γ, or -δ does not affect endothelial junctions or morphology. Fig. S3 shows that depletion of p110 isoforms does not affect the expression of junctional proteins or TNF-induced p38MAPK activation. Fig. S4 shows that depletion of p110β, -γ, or -δ does not affect junctional organization or ICAM-1 clustering in TNF-stimulated cells. Fig. S5 shows the effects of p110, Rac1, and RhoA depletion on endothelial junctions. Online supplemental material is available at http://www.jcb.org/cgi/content/full/jcb.200907135/DC1.

We thank Eva Cernuda-Morollon for purified T cells, Sarah Heasman for her advice on T-cell culture, Mariona Graupera for advice on PI3Ks, and Brian Stramer for the use of Volocity image software. We are also grateful to Ferran Valderrama, Virginia Tajadura, and Nicolas Reymond for discussions.

This work was funded by the Association for International Cancer Research (grant to A.J. Ridley), Cancer Research UK (grant to A.J. Ridley and B. Vanhaesebroeck), Biotechnology and Biological Sciences Research Council (grant to A.J. Ridley and B. Vanhaesebroeck), European Commission Framework 6 contract no. LSHG-CT-2003-502935 (to A.J. Ridley and B. Vanhaesebroeck), and Bettencourt-Schueller Foundation (grant to A.J. Ridley).

Submitted: 23 July 2009
Accepted: 25 February 2010

References

Aghajanian, A., E.S. Wittchen, M.J. Allingham, T.A. Garrett, and K. Burridge. 2008. Endothelial cell junctions and the regulation of vascular permeability and leukocyte transmigration. *J. Thromb. Haemost.* 6:1453–1460. doi:10.1111/j.1538-7836.2008.03087.x

Allingham, M.J., J.D. van Buul, and K. Burridge. 2007. ICAM-1-mediated, Src- and Pyk2-dependent vascular endothelial cadherin tyrosine phosphorylation is required for leukocyte transendothelial migration. *J. Immunol.* 179:4053–4064.

Angelini, D.J., S.W. Hyun, D.N. Grigoryev, P. Garg, P. Gong, I.S. Singh, A. Passaniti, J.D. Hasday, and S.E. Goldblum. 2006. TNF-α increases tyrosine phosphorylation of vascular endothelial cadherin and opens the paracellular pathway through fyn activation in human lung endothelia. *Am. J. Physiol. Lung Cell. Mol. Physiol.* 291:L1232–L1245. doi:10.1152/ajplung.00109.2006

Barreiro, O., M. Yanez-Mo, J.M. Serrador, M.C. Montoya, M. Vicente-Manzanares, R. Tejedor, H. Furthmayr, and F. Sanchez-Madrid. 2002. Dynamic interaction of VCAM-1 and ICAM-1 with moesin and ezrin in a novel endothelial docking structure for adherent leukocytes. *J. Cell Biol.* 157:1233–1245. doi:10.1083/jcb.200112126

Basile, J.R., J. Gavard, and J.S. Gutkind. 2007. Plexin-B1 utilizes RhoA and Rho kinase to promote the integrin-dependent activation of Akt and ERK and endothelial cell motility. *J. Biol. Chem.* 282:34888–34895. doi:10.1074/jbc.M705467200

Bäumer, S., L. Keller, A. Holtmann, R. Funke, B. August, A. Gamp, H. Wolburg, K. Wolburg-Buchholz, U. Deutsch, and D. Vestweber. 2006. Vascular endothelial cell-specific phosphotyrosine phosphatase (VE-PTP) activity is required for blood vessel development. *Blood*. 107:4754–4762. doi:10.1182/blood-2006-01-0141

Birukov, K.G. 2009. Small GTPases in mechanosensitive regulation of endothelial barrier. *Microvasc. Res.* 77:46–52. doi:10.1016/j.mvr.2008.09.006

Birukova, A.A., K.G. Birukov, B. Gorshkov, F. Liu, J.G. Garcia, and A.D. Verin. 2005. MAP kinases in lung endothelial permeability induced by microtubule disassembly. *Am. J. Physiol. Lung Cell. Mol. Physiol.* 289:L75–L84. doi:10.1152/ajplung.00447.2004

Bruewer, M., A.M. Hopkins, M.E. Hobert, A. Nusrat, and J.L. Madara. 2004. RhoA, Rac1, and Cdc42 exert distinct effects on epithelial barrier via selective structural and biochemical modulation of junctional proteins and F-actin. *Am. J. Physiol. Cell Physiol.* 287:C327–C335. doi:10.1152/ajpcell.00087.2004

Cain, R.J., and A.J. Ridley. 2009. Phosphoinositide 3-kinases in cell migration. *Biol. Cell*. 101:13–29. doi:10.1042/BC20080079

Carman, C.V., and T.A. Springer. 2004. A transmigratory cup in leukocyte diapedesis both through individual vascular endothelial cells and between them. *J. Cell Biol.* 167:377–388. doi:10.1083/jcb.200404129

Carmeliet, P., M.G. Lampugnani, L. Moons, F. Breviario, V. Compernolle, F. Bono, G. Balconi, R. Spagnuolo, B. Oosthuyse, M. Dewerchin, et al. 1999. Targeted deficiency or cytosolic truncation of the VE-cadherin gene in mice impairs VEGF-mediated endothelial survival and angiogenesis. *Cell*. 98:147–157. doi:10.1016/S0092-8674(00)81010-7

Corada, M., M. Mariotti, G. Thurston, K. Smith, R. Kunkel, M. Brockhaus, M.G. Lampugnani, I. Martin-Padura, A. Stoppacciaro, L. Ruco, et al. 1999. Vascular endothelial-cadherin is an important determinant of microvascular integrity in vivo. *Proc. Natl. Acad. Sci. USA*. 96:9815–9820. doi:10.1073/pnas.96.17.9815

Cotran, R.S., and J.S. Pober. 1990. Cytokine-endothelial interactions in inflammation, immunity, and vascular injury. *J. Am. Soc. Nephrol.* 1:225–235.

Dejana, E., F. Orsenigo, and M.G. Lampugnani. 2008. The role of adherens junctions and VE-cadherin in the control of vascular permeability. *J. Cell Sci.* 121:2115–2122. doi:10.1242/jcs.017897

Engelhardt, B., and H. Wolburg. 2004. Mini-review: Transendothelial migration of leukocytes: through the front door or around the side of the house? *Eur. J. Immunol.* 34:2955–2963. doi:10.1002/eji.200425327

Esser, S., M.G. Lampugnani, M. Corada, E. Dejana, and W. Risau. 1998. Vascular endothelial growth factor induces VE-cadherin tyrosine phosphorylation in endothelial cells. *J. Cell Sci.* 111:1853–1865.

Essler, M., K. Hermann, M. Amano, K. Kaibuchi, J. Heesemann, P.C. Weber, and M. Aepfelbacher. 1998. Pasteurella multocida toxin increases endothelial permeability via Rho kinase and myosin light chain phosphatase. *J. Immunol.* 161:5640–5646.

Fryer, B.H., and J. Field. 2005. Rho, Rac, Pak and angiogenesis: old roles and newly identified responsibilities in endothelial cells. *Cancer Lett.* 229:13–23. doi:10.1016/j.canlet.2004.12.009

Gavard, J., X. Hou, Y. Qu, A. Masedunskas, D. Martin, R. Weigert, X. Li, and J.S. Gutkind. 2009. A role for a CXCR2/phosphatidylinositol 3-kinase γ signaling axis in acute and chronic vascular permeability. *Mol. Cell. Biol.* 29:2469–2480. doi:10.1128/MCB.01304-08

Graupera, M., J. Guillermet-Guibert, L.C. Foukas, L.K. Phng, R.J. Cain, A. Salpekar, W. Pearce, S. Meek, J. Millan, P.R. Cutillas, et al. 2008. Angiogenesis selectively requires the p110α isoform of PI3K to control endothelial cell migration. *Nature*. 453:662–666. doi:10.1038/nature06892

Guillermet-Guibert, J., K. Bjorklof, A. Salpekar, C. Gonella, F. Ramadani, A. Bilancio, S. Meek, A.J. Smith, K. Okkenhaug, and B. Vanhaesebroeck. 2008. The p110β isoform of phosphoinositide 3-kinase signals downstream of G protein-coupled receptors and is functionally redundant with p110γ. *Proc. Natl. Acad. Sci. USA*. 105:8292–8297. doi:10.1073/pnas.0707761105

Gumbiner, B.M. 2005. Regulation of cadherin-mediated adhesion in morphogenesis. *Nat. Rev. Mol. Cell Biol.* 6:622–634. doi:10.1038/nrm1699

Hordijk, P.L., J.P. ten Klooster, R.A. van der Kammen, F. Michiels, L.C. Oomen, and J.G. Collard. 1997. Inhibition of invasion of epithelial cells by Tiam1-Rac signaling. *Science*. 278:1464–1466. doi:10.1126/science.278.5342.1464

Hordijk, P.L., E. Anthony, F.P. Mul, R. Rientsma, L.C. Oomen, and D. Roos. 1999. Vascular-endothelial-cadherin modulates endothelial monolayer permeability. *J. Cell Sci.* 112:1915–1923.

Hu, G., and R.D. Minshall. 2009. Regulation of transendothelial permeability by Src kinase. *Microvasc. Res.* 77:21–25. doi:10.1016/j.mvr.2008.10.002

Hudry-Clergeon, H., D. Stengel, E. Ninio, and I. Vilgrain. 2005. Platelet-activating factor increases VE-cadherin tyrosine phosphorylation in mouse endothelial cells and its association with the PtdIns3′-kinase. *FASEB J.* 19:512–520. doi:10.1096/fj.04-2202com

Kilic, E., U. Kilic, Y. Wang, C.L. Bassetti, H.H. Marti, and D.M. Hermann. 2006. The phosphatidylinositol-3 kinase/Akt pathway mediates VEGF's neuroprotective activity and induces blood brain barrier permeability after focal cerebral ischemia. *FASEB J.* 20:1185–1187. doi:10.1096/fj.05-4829fje

Lambeng, N., Y. Wallez, C. Rampon, F. Cand, G. Christé, D. Gulino-Debrac, I. Vilgrain, and P. Huber. 2005. Vascular endothelial-cadherin tyrosine phosphorylation in angiogenic and quiescent adult tissues. *Circ. Res.* 96:384–391. doi:10.1161/01.RES.0000156652.99586.9f

Lampugnani, M.G., M. Corada, L. Caveda, F. Breviario, O. Ayalon, B. Geiger, and E. Dejana. 1995. The molecular organization of endothelial cell to cell junctions: differential association of plakoglobin, beta-catenin, and alpha-catenin with vascular endothelial cadherin (VE-cadherin). *J. Cell Biol.* 129:203–217. doi:10.1083/jcb.129.1.203

Lampugnani, M.G., A. Zanetti, F. Breviario, G. Balconi, F. Orsenigo, M. Corada, R. Spagnuolo, M. Betson, V. Braga, and E. Dejana. 2002. VE-cadherin regulates endothelial actin activating Rac and increasing membrane association of Tiam. *Mol. Biol. Cell*. 13:1175–1189. doi:10.1091/mbc.01-07-0368

Li, Y., L. Sun, H. Xu, Z. Fang, W. Yao, W. Guo, J. Rao, and X. Zha. 2008. Angiopoietin-like protein 3 modulates barrier properties of human glomerular endothelial cells through a possible signaling pathway involving phosphatidylinositol-3 kinase/protein kinase B and integrin alphaVbeta3. *Acta Biochim. Biophys. Sin. (Shanghai)*. 40:459–465. doi:10.1111/j.1745-7270.2008.00421.x

McKenzie, J.A., and A.J. Ridley. 2007. Roles of Rho/ROCK and MLCK in TNF-α-induced changes in endothelial morphology and permeability. *J. Cell. Physiol.* 213:221–228. doi:10.1002/jcp.21114

Melikova, S.V., S.J. Dylla, and C.M. Verfaillie. 2004. Phosphatidylinositol-3-kinase activation mediates proline-rich tyrosine kinase 2 phosphorylation and recruitment to beta1-integrins in human CD34+ cells. *Exp. Hematol.* 32:1051–1056. doi:10.1016/j.exphem.2004.07.018

Michiels, F., J.C. Stam, P.L. Hordijk, R.A. van der Kammen, L. Ruuls-Van Stalle, C.A. Feltkamp, and J.G. Collard. 1997. Regulated membrane localization of Tiam1, mediated by the NH_2-terminal pleckstrin homology domain, is required for Rac-dependent membrane ruffling and C-Jun NH_2-terminal kinase activation. *J. Cell Biol.* 137:387–398. doi:10.1083/jcb.137.2.387

Millán, J., and A.J. Ridley. 2005. Rho GTPases and leucocyte-induced endothelial remodelling. *Biochem. J.* 385:329–337. doi:10.1042/BJ20041584

Millán, J., L. Hewlett, M. Glyn, D. Toomre, P. Clark, and A.J. Ridley. 2006. Lymphocyte transcellular migration occurs through recruitment of endothelial ICAM-1 to caveola- and F-actin-rich domains. *Nat. Cell Biol.* 8:113–123. doi:10.1038/ncb1356

Mitra, S.K., D.A. Hanson, and D.D. Schlaepfer. 2005. Focal adhesion kinase: in command and control of cell motility. *Nat. Rev. Mol. Cell Biol.* 6:56–68. doi:10.1038/nrm1549

Nakhaei-Nejad, M., A.M. Hussain, Q.-X. Zhang, and A.G. Murray. 2007. Endothelial PI 3-kinase activity regulates lymphocyte diapedesis. *Am. J. Physiol. Heart Circ. Physiol.* 293:H3608–H3616. doi:10.1152/ajpheart.00321.2007

Noria, S., D.B. Cowan, A.I. Gotlieb, and B.L. Langille. 1999. Transient and steady-state effects of shear stress on endothelial cell adherens junctions. *Circ. Res.* 85:504–514.

Nourshargh, S., and F.M. Marelli-Berg. 2005. Transmigration through venular walls: a key regulator of leukocyte phenotype and function. *Trends Immunol.* 26:157–165. doi:10.1016/j.it.2005.01.006

Papakonstanti, E.A., A.J. Ridley, and B. Vanhaesebroeck. 2007. The p110δ isoform of PI 3-kinase negatively controls RhoA and PTEN. *EMBO J.* 26:3050–3061. doi:10.1038/sj.emboj.7601763

Parsons, S.J., and J.T. Parsons. 2004. Src family kinases, key regulators of signal transduction. *Oncogene*. 23:7906–7909. doi:10.1038/sj.onc.1208160

Potter, M.D., S. Barbero, and D.A. Cheresh. 2005. Tyrosine phosphorylation of VE-cadherin prevents binding of p120- and β-catenin and maintains the cellular mesenchymal state. *J. Biol. Chem.* 280:31906–31912. doi:10.1074/jbc.M505568200

Puri, K.D., T.A. Doggett, J. Douangpanya, Y. Hou, W.T. Tino, T. Wilson, T. Graf, E. Clayton, M. Turner, J.S. Hayflick, and T.G. Diacovo. 2004. Mechanisms and implications of phosphoinositide 3-kinase δ in promoting neutrophil trafficking into inflamed tissue. *Blood*. 103:3448–3456. doi:10.1182/blood-2003-05-1667

Puri, K.D., T.A. Doggett, C.Y. Huang, J. Douangpanya, J.S. Hayflick, M. Turner, J. Penninger, and T.G. Diacovo. 2005. The role of endothelial PI3Kgamma activity in neutrophil trafficking. *Blood*. 106:150–157. doi:10.1182/blood-2005-01-0023

Sander, E.E., S. van Delft, J.P. ten Klooster, T. Reid, R.A. van der Kammen, F. Michiels, and J.G. Collard. 1998. Matrix-dependent Tiam1/Rac signaling in epithelial cells promotes either cell-cell adhesion or cell migration and is regulated by phosphatidylinositol 3-kinase. *J. Cell Biol.* 143:1385–1398. doi:10.1083/jcb.143.5.1385

Serban, D., J. Leng, and D. Cheresh. 2008. H-ras regulates angiogenesis and vascular permeability by activation of distinct downstream effectors. *Circ. Res.* 102:1350–1358. doi:10.1161/CIRCRESAHA.107.169664

Shasby, D.M., D.R. Ries, S.S. Shasby, and M.C. Winter. 2002. Histamine stimulates phosphorylation of adherens junction proteins and alters their link to vimentin. *Am. J. Physiol. Lung Cell. Mol. Physiol.* 282:L1330–L1338.

Stolpen, A.H., E.C. Guinan, W. Fiers, and J.S. Pober. 1986. Recombinant tumor necrosis factor and immune interferon act singly and in combination to reorganize human vascular endothelial cell monolayers. *Am. J. Pathol.* 123:16–24.

Suire, S., J. Coadwell, G.J. Ferguson, K. Davidson, P. Hawkins, and L. Stephens. 2005. p84, a new Gbetagamma-activated regulatory subunit of the type IB phosphoinositide 3-kinase p110γ. *Curr. Biol.* 15:566–570. doi:10.1016/j.cub.2005.02.020

Turowski, P., R. Martinelli, R. Crawford, D. Wateridge, A.P. Papageorgiou, M.G. Lampugnani, A.C. Gamp, D. Vestweber, P. Adamson, E. Dejana, and J. Greenwood. 2008. Phosphorylation of vascular endothelial cadherin controls lymphocyte emigration. *J. Cell Sci.* 121:29–37. doi:10.1242/jcs.022681

Tzima, E. 2006. Role of small GTPases in endothelial cytoskeletal dynamics and the shear stress response. *Circ. Res.* 98:176–185. doi:10.1161/01.RES.0000200162.94463.d7

van Buul, J.D., E.C. Anthony, M. Fernandez-Borja, K. Burridge, and P.L. Hordijk. 2005. Proline-rich tyrosine kinase 2 (Pyk2) mediates vascular endothelial-cadherin-based cell-cell adhesion by regulating β-catenin tyrosine phosphorylation. *J. Biol. Chem.* 280:21129–21136. doi:10.1074/jbc.M500898200

van Gils, J.M., J. Stutterheim, T.J. van Duijn, J.J. Zwaginga, L. Porcelijn, M. de Haas, and P.L. Hordijk. 2009. HPA-1a alloantibodies reduce endothelial cell spreading and monolayer integrity. *Mol. Immunol.* 46:406–415. doi:10.1016/j.molimm.2008.10.015

van Wetering, S., N. van den Berk, J.D. van Buul, F.P. Mul, I. Lommerse, R. Mous, J.P. ten Klooster, J.J. Zwaginga, and P.L. Hordijk. 2003. VCAM-1-mediated Rac signaling controls endothelial cell-cell contacts and leukocyte transmigration. *Am. J. Physiol. Cell Physiol.* 285:C343–C352.

Vanhaesebroeck, B., and D.R. Alessi. 2000. The PI3K-PDK1 connection: more than just a road to PKB. *Biochem. J.* 346:561–576. doi:10.1042/0264-6021:3460561

Vanhaesebroeck, B., S.J. Leevers, K. Ahmadi, J. Timms, R. Katso, P.C. Driscoll, R. Woscholski, P.J. Parker, and M.D. Waterfield. 2001. Synthesis and function of 3-phosphorylated inositol lipids. *Annu. Rev. Biochem.* 70:535–602. doi:10.1146/annurev.biochem.70.1.535

Vouret-Craviari, V., P. Boquet, J. Pouysségur, and E. Van Obberghen-Schilling. 1998. Regulation of the actin cytoskeleton by thrombin in human endothelial cells: role of Rho proteins in endothelial barrier function. *Mol. Biol. Cell*. 9:2639–2653.

Wallez, Y., F. Cand, F. Cruzalegui, C. Wernstedt, S. Souchelnytskyi, I. Vilgrain, and P. Huber. 2007. Src kinase phosphorylates vascular endothelial-cadherin in response to vascular endothelial growth factor: identification of tyrosine 685 as the unique target site. *Oncogene*. 26:1067–1077. doi:10.1038/sj.onc.1209855

Weis, S., S. Shintani, A. Weber, R. Kirchmair, M. Wood, A. Cravens, H. McSharry, A. Iwakura, Y.S. Yoon, N. Himes, et al. 2004. Src blockade stabilizes a Flk/cadherin complex, reducing edema and tissue injury following myocardial infarction. *J. Clin. Invest.* 113:885–894.

Wojciak-Stothard, B., and A.J. Ridley. 2002. Rho GTPases and the regulation of endothelial permeability. *Vascul. Pharmacol.* 39:187–199. doi:10.1016/S1537-1891(03)00008-9

Wójciak-Stothard, B., A. Entwistle, R. Garg, and A.J. Ridley. 1998. Regulation of TNF-α-induced reorganization of the actin cytoskeleton and cell-cell junctions by Rho, Rac, and Cdc42 in human endothelial cells. *J. Cell. Physiol.* 176:150–165. doi:10.1002/(SICI)1097-4652(199807)176:1<150::AID-JCP17>3.0.CO;2-B

Yuan, T.L., H.S. Choi, A. Matsui, C. Benes, E. Lifshits, J. Luo, J.V. Frangioni, and L.C. Cantley. 2008. Class 1A PI3K regulates vessel integrity during development and tumorigenesis. *Proc. Natl. Acad. Sci. USA*. 105:9739–9744. doi:10.1073/pnas.0804123105